Supplemental Material for "Electric polarization of soft biological tissues induced by ultrasound waves"

Kenji Ikushima, Takashi Kumamoto, Kenshiro Ito, and Yamato Anzai
Department of Biomedical Engineering, Tokyo University of Agriculture and Technology, Nakacho, Koganei, Tokyo 184-8588, Japan

A. Sample preparation

Fresh biological specimens were harvested from a slaughterhouse through a livestock organ sales company (Funakoshi Co., Ltd.). These specimens were extracted under the supervision of the veterinarian. Immediately after delivery, the specimens were frozen at -20 °C. Before performing experiments, the specimens were thawed and rinsed in deionized water. Bovine Achilles tendon was cut to the specified size ($12 \times 10 \times 6$ mm) by the company; all other tissues were cut in the lab. Figure S1 shows the sample extraction procedure for the aortic valve tissue. Aortic valve samples about $10 \times 20 \times 4$ mm were cut from a specimen consisting of myocardium, aortic wall, and aortic valve. A piece of myocardium was also used for the measurements. Samples of aortic wall were cut from the middle section of the other long aorta.

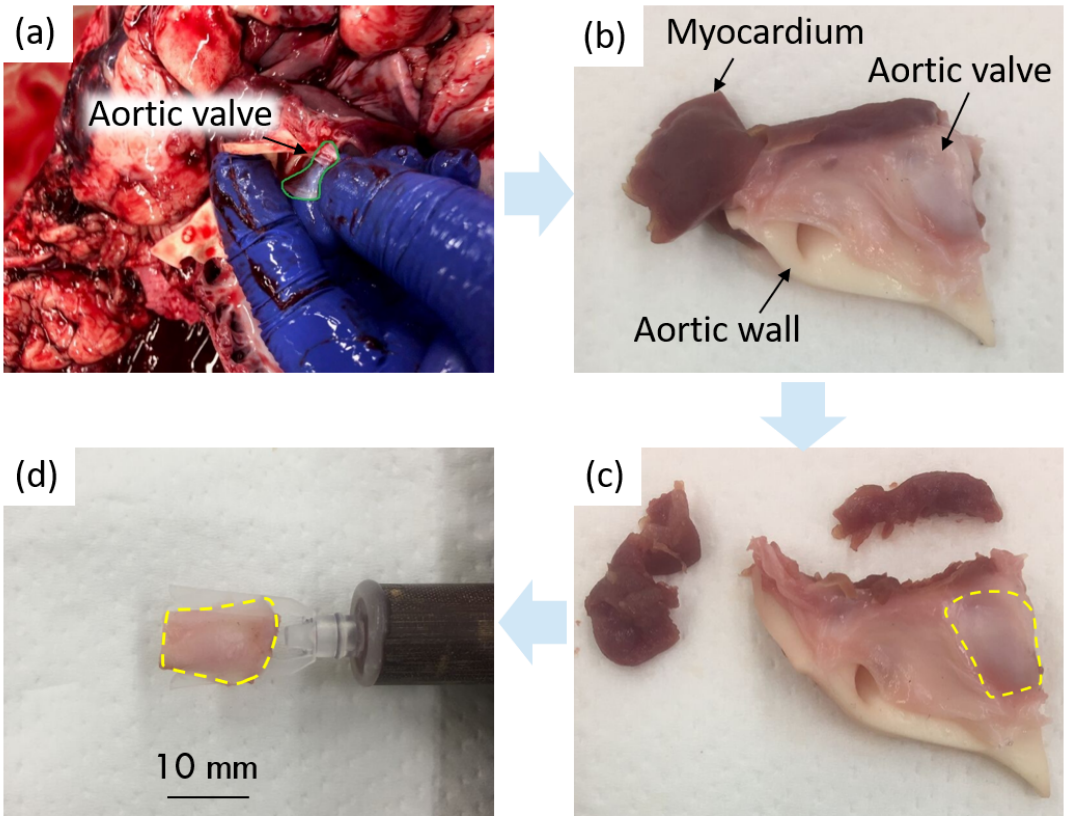

FIG. S1: Photograph of (a) the aortic valve in a porcine heart, (b), (c) extracted aortic tissue consisting of the myocardium, aortic valve, and aortic wall, and (d) the aortic valve sample set in a sample holder.

B. Acoustically induced electric polarization and alternating electric dipole field

Under adiabatic conditions, the applicable mechanical and electric equations of state for the piezoelectric medium can be written as ($i, j = 1, 2, \ldots, 6$, and $k, m = 1, 2, 3$)

$$\begin{aligned} S_i &= s_{ij} T_j + d_{mi} E_m, \\ D_m &= d_{mi} T_i + \epsilon_{mk} E_k, \end{aligned} \tag{1}$$

where S, T, E, and D are the strain, stress, electric field, and electric flux density components, respectively. The coefficients relating the quantities s_{ij}, d_{mi}, and ϵ_{mk} are the elastic compliance, piezoelectric constant, and dielectric constant, respectively. Electrostriction is phenomenologically equivalent to piezoelectricity in the linear response regime, and we make no distinction between them for the purpose of this discussion [26]. The local flux density, $D_m(t)$ (or electric polarization $P_m(t)$), is temporally modulated through Eq. (1) when stress $T_i(t)$ is applied locally by ultrasound irradiation. Consequently, the first harmonic component of locally induced polarization, $\boldsymbol{P}_m = \sum_{i=1}^{6} d_{mi} T_i = \overline{\boldsymbol{p}}(t)/V$, oscillates at the ultrasound frequency, where $\overline{\boldsymbol{p}}(t)$ is a summation of electric dipole moment $\sum_l \boldsymbol{p}_l(t)$ produced by aggregations of partially oriented or quasi-crystalline regions in the acoustically excited area S_{ex}, V is the excited volume $S_{\mathrm{ex}} \cdot |\boldsymbol{l}|$, and $\boldsymbol{l}$ is the displacement vector pointing between opposite effective charges, $\pm q_{\mathrm{dip}}$. $|\boldsymbol{l}|$ is on the order of the half wavelength of ultrasound waves (75 μm at 10 MHz in water). The alternating electric dipole field emitted to the surrounding environment is then expressed as

$$\boldsymbol{E}_{\mathrm{dip}}(\boldsymbol{x}, t) = \frac{1}{4\pi\epsilon_0} \frac{3\boldsymbol{n}_0(\boldsymbol{n}_0 \cdot \overline{\boldsymbol{p}}(t)) - \overline{\boldsymbol{p}}(t)}{r^3}, \tag{2}$$

where $\boldsymbol{x} = \boldsymbol{n}_0 r$ represents a vector from the position of the electric dipole moment to the observation point with a distance of r (on the order of centimeters) and ϵ_0 is the vacuum permittivity. This acoustically induced electric field, which corresponds to ASEM response, is detected by using a resonant capacitive antenna.

C. Charge detection model

Because $r \gg |\boldsymbol{l}|$, we first assume a simple charge detection model. Suppose that a surface charge, $Q(t) = Q_0 \sin \omega_0 t$, is induced on a disk-shaped metal plate with radius R by an effective charge, $q(t) = q_{\mathrm{eff}} \sin \omega_0 t$, on biological tissues (Fig. S2), where ω_0 is the center frequency of the LCR resonator tuned to the ultrasound frequency. Using the image charges method, the electrostatic potential is written as $V(x_1, x_2, x_3) = q_{\mathrm{eff}}(1/r - 1/r')/(4\pi\epsilon_0)$, where r (r') is the distance between a given observation point and the position of the charge, $+q_{\mathrm{eff}}$ (the mirror charge is $-q_{\mathrm{eff}}$). Thus, the electric field generated at point A on the metal antenna is expressed by

$$E_{\mathrm{charge}} = -\left.\frac{\partial V}{\partial x_1}\right|_{x_1=0} = -\frac{1}{4\pi\epsilon_0} \frac{2q_{\mathrm{eff}}}{r_{\mathrm{A}}^2} \left(\frac{h}{r_{\mathrm{A}}}\right), \tag{3}$$

where $r_{\mathrm{A}} = \sqrt{a^2 + h^2}$ is the distance between the charge and point A, and a is the radial coordinate, $\sqrt{x_2^2 + x_3^2}$, of the metal disk (Fig. S2). Accordingly, the surface charge density, $\sigma = \epsilon_0 E_{\mathrm{charge}}$, is induced on the metal plate. Thus,

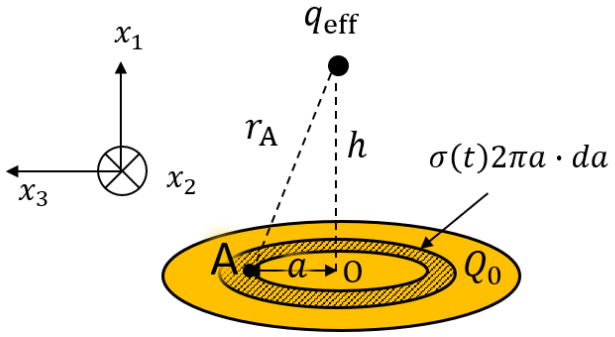

FIG. S2: Schematic of the charge detection model

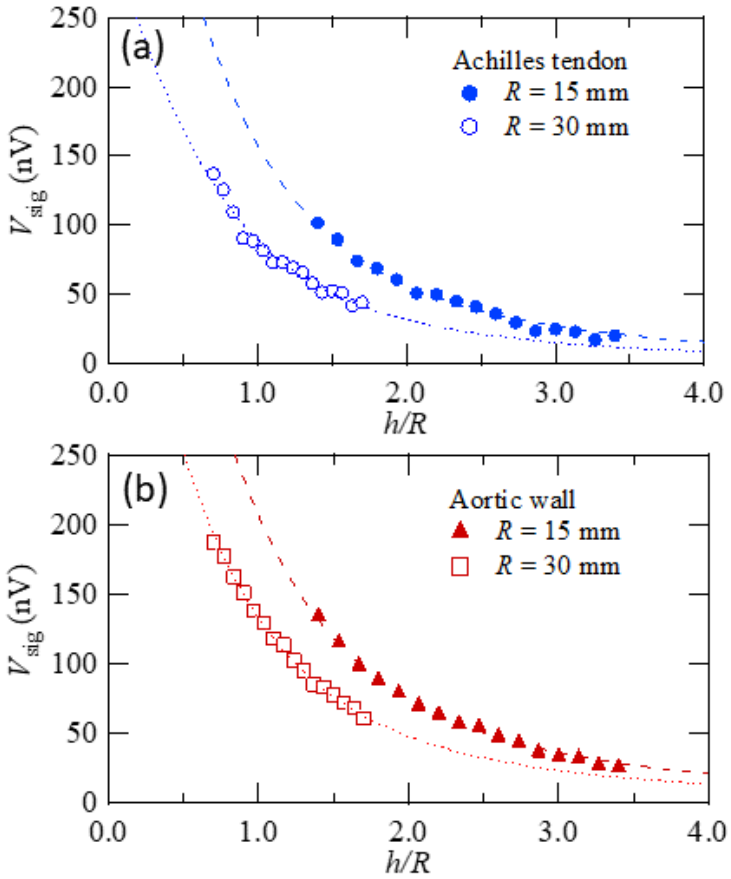

FIG. S3: $V_{\rm sig}$ versus h/R for Achilles tendon and aortic wall, respectively. The dashed and dotted lines represent the best-fit curves based on the charge detection model for $R = 15$ and 30 mm, respectively.

the total charge, Q_0, is written for an annular portion, $2\pi a \cdot da$, with a width of da as

$$\begin{aligned} Q_0 &= \int_0^R \sigma \cdot 2\pi a \cdot da \\ &= -q_{\rm eff}\left[1 - \frac{(h/R)}{\sqrt{1+(h/R)^2}}\right], \end{aligned} \tag{4}$$

where $Q_0 \to -q_{\rm eff}$ for $h/R \to 0$. The derivative of the surface charge, dQ/dt, flows as an alternating electric current, $i(t)$, in the LCR resonator tuned to ω_0. The electric current is converted to the amplitude of the signal voltage, $V_{\rm sig}$, through the input impedance of the preamplifier, $Z_{\rm in} = 50\ \Omega$. Thus, the signal voltage $V_{\rm sig}(t)$ is obtained from $Z_{\rm in} \cdot (dQ/dt)/2 = Z_{\rm in}\omega_0 Q(t)/2$. Therefore, the voltage amplitude of the ASEM signal, $V_{\rm sig}$, is also expressed by

$$V_{\rm sig} = V_0\left[1 - \frac{(h/R)}{\sqrt{1+(h/R)^2}}\right], \tag{5}$$

where V_0 corresponds to the signal amplitude for $h/R \to 0$. Consequently, using V_0 evaluated from an experimental value of $V_{\rm sig}$ for a given h/R, the induced charge is obtained by $q_{\rm eff} = 2V_0/(Z_{\rm in}\omega_0)$.

The h/R-dependence of $V_{\rm sig}$ for Achilles tendon and aorta wall is shown in Figs. S3(a) and S3(b), respectively, where the signals are detected by using two antennas with $R = 15$ and 30 mm. The experimental data are well fitted to Eq. (10), and V_0 for $R = 15$ mm is evaluated to be 540 and 700 nV for Achilles tendon and aortic wall, respectively. The effective charge is estimated to be $q_{\rm eff} = 4.0 \times 10^{-16}$ C and $q_{\rm eff} = 5.1 \times 10^{-16}$ C for Achilles tendon and aortic wall, respectively, which correspond to a charge amount of about 10^3 electrons. We note that the h/R-curve is shifted when the antenna radius R is different. This charge detection model is insufficient for quantitative evaluation of the induced charge.

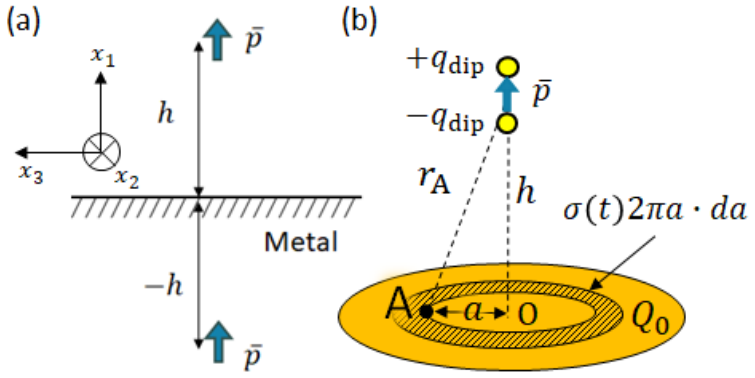

FIG. S4: Schematics of the (a) image dipole and (b) dipole detection model.

D. Dipole detection model

Considering the requirement of charge neutrality, the acoustically induced charge, q_{eff}, results from the electric dipole. The electric dipole field is approximately equivalent to an electric field generated by an effective charge when the antenna is sufficiently far from the dipole. However, the effective charge should be much smaller than the net polarization charge, q_{dip}, because it is only the amount that cannot be cancelled by positive and negative charges. The electric dipole field, E_{dip}, at the center of the antenna can be expressed by $\left(2q_{\mathrm{dip}}/h^2\right)(l/h)/(4\pi\epsilon_0)$, where the direction of polarization is perpendicular to the surface of the antenna. The ratio of the electric field is $|E_{\mathrm{dip}}|/|E_{\mathrm{charge}}| \simeq |q_{\mathrm{dip}}/q_{\mathrm{eff}}| \cdot (l/h)$. Therefore, the polarization charge, q_{dip}, can be approximated by $q_{\mathrm{eff}} \cdot (h/l)$. Using $l \sim 0.1$ mm and $h = 21$ mm, q_{dip} is roughly two orders of magnitude larger than the value of q_{eff}. Thus, we extend the model described in Sec. C to the dipole detection model. Suppose that a surface charge, $Q(t) = Q_0 \sin\omega_0 t$, is induced on a metal plate by an electric dipole moment, $\bar{p} = q_{\mathrm{dip}} l$ (Fig. S4). Using the image dipole method (Fig. S4(a)), the electrostatic potential arising from the dipole moment is written as

$$V(x_1, x_2, x_3) = -\frac{1}{4\pi\epsilon_0}\left[\frac{\bar{p}(h - x_1)}{\{(x_1 - h)^2 + x_2^2 + x_3^2\}^{3/2}} + \frac{-\bar{p}(x_1 + h)}{\{(x_1 + h)^2 + x_2^2 + x_3^2\}^{3/2}}\right], \tag{6}$$

where h is the distance between the dipole and the metal plate ($h \gg l$). Thus, the electric field generated at point A on the metal surface (Fig. S4(b)) is expressed by

$$E_1(0, x_2, x_3) = -\left.\frac{\partial V}{\partial x_1}\right|_{x_1=0} = -\frac{\bar{p}}{2\pi\epsilon_0}\frac{a^2 - 2h^2}{r_A^5}. \tag{7}$$

The total charge, Q_0, induced on the metal plate of radius R is written as

$$\begin{aligned} Q_0 &= \int_0^R \sigma \cdot 2\pi a \cdot da \\ &= \frac{\bar{p}}{R}\left[1 + (h/R)^2\right]^{-3/2}. \end{aligned} \tag{8}$$

The total charge, Q_0, multiplied by R is expressed as a function of a single variable, h/R, by

$$Q_0 \times R = q_{\mathrm{dip}} l \left[1 + (h/R)^2\right]^{-3/2}. \tag{9}$$

The derivative of the surface charge, dQ/dt, flows as an alternating electric current, $i(t)$, in the LCR resonator tuned to ω_0. The electric current is converted to the amplitude of the signal voltage, V_{sig}, through the input impedance of the preamplifier, $Z_{\mathrm{in}} = 50\ \Omega$. Using $V_{\mathrm{sig}} = Z_{\mathrm{in}}\omega_0 Q_0/2$, the voltage amplitude of the ASEM signal, V_{sig}, is also expressed as a function of the single variable, h/R, by

$$\begin{aligned} V_{\mathrm{sig}} \times R &= \frac{q_{\mathrm{dip}} l Z_{\mathrm{in}}\omega_0}{2}\left[1 + (h/R)^2\right]^{-3/2} \\ &= V_0 R\left[1 + (h/R)^2\right]^{-3/2}, \end{aligned} \tag{10}$$

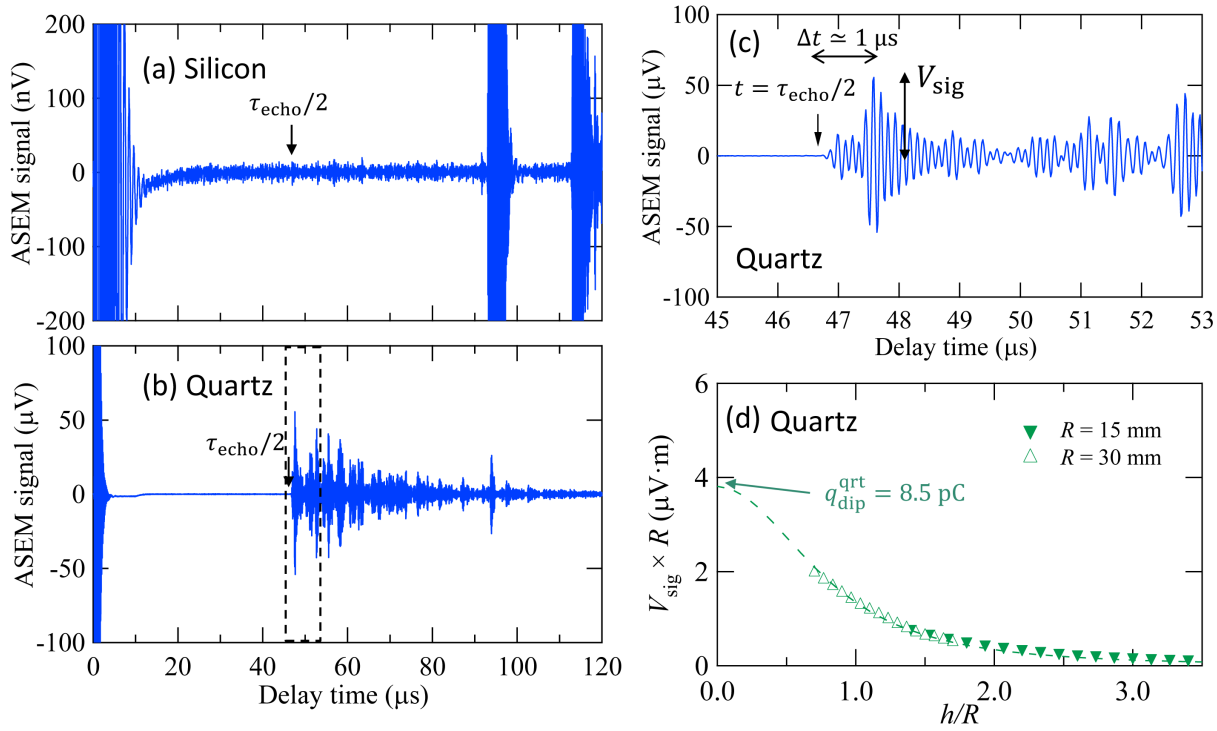

FIG. S5: Time traces of ASEM signals in (a) a nonpiezoelectric silicon crystal (a 3 inch nondoped Si(100) wafer, thickness: 0.38 mm) and (b) a piezoelectric quartz crystal (AT cut, diameter: 12.4 mm, thickness: 0.33 mm). (c) Expanded time trace of ASEM signals around $\tau_{echo}/2$ in quartz. The ASEM signal is generated with a delay time of $\Delta t \simeq 1\mu$s. (d) The h/R dependence of $V_{sig} \times R$ exhibits the scaling behavior with respect to R in quartz.

where V_0 corresponds to the signal amplitude for $h/R \to 0$ and $V_0 R$ is independent of the antenna radius, R. The scaling behavior in $V_{sig} \times R$ versus h/R with respect to different R (Fig. 6(b)) strongly supports the dipole detection model and provides convincing evidence for the presence of stress-induced polarization.

E. Estimation of piezoelectric coefficients

The ASEM signal detected in soft biological tissues is well explained by the dipole detection model. However, the quantitative analysis of piezoelectric coefficients is not easy because of the limit of the simplified model. In the dipole detection model, the following parameters are unknown: the acoustically excited area (the area of polarization), S_{ex}, and the length of polarization (the displacement between opposite effective charges, $\pm q_{dip}$), l. To verify the quantitative accuracy for piezoelectric coefficients, we measured ASEM signals in a nonpiezoelectric silicon crystal (Fig. S5(a)) and a piezoelectric quartz crystal (Fig. S5(b)). No explicit signal was observed in silicon, whereas a large signal was observed in quartz. The similar results are also reported for silicon and piezoelectric GaAs in Ref. [18]. These results support that the ASEM signal is attributed to the piezoelectricity. The ASEM waveform in quartz is complicated owing to the generation of several acoustic modes. Around $t = \tau_{echo}/2$, the signal exhibits a time delay of $\Delta t \simeq 1\mu$s which corresponds to a propagation length of about 6 mm (sample radius) using a ultrasound velocity of 6000 m/s in quartz (Fig.S5(c)). This means that the longitudinal wave irradiated on the focal spot ($\Delta r = 0.65$ mm) is converted to a thickness mode of the whole crystal after $t = \tau_{echo}/2 + \Delta t$ and the signal is enhanced by the mechanical resonance. Therefore, S_{ex} and l will be the whole area of the sample surface (1.2×10^{-4} m^2) and the sample thickness (0.33 mm), respectively.

The scaling behavior in $V_{sig} \times R$ versus h/R with respect to different R was observed in the quartz crystal, supporting the dipole detection model (Fig. S5(d)). From the value for $h/R \to 0$, the induced polarization charge is estimated to be $q_{dip}^{qrt} = 8.5$ pC. Thus, the piezoelectric coefficient is estimated to be 22 pC/N, which is about one order of magnitude larger than the reported value ~ 2 pC/N [27]. One possibility for this difference is that the signal is enhanced by the mechanical resonance of high-Q materials. In the resonance condition, the applied broad-band ultrasound energy

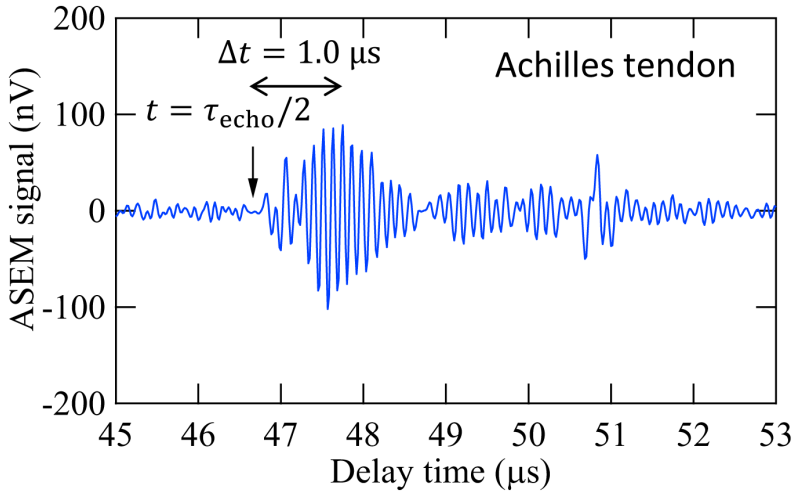

FIG. S6: Expanded time trace of ASEM signals around $\tau_{\mathrm{echo}}/2$ in Achilles tendon.

is concentrated to the mechanical oscillation at the resonance frequency through mode conversions and the energy is accumulated in the crystal over several periods. The signal enhancement due to the mechanical resonance is also reported in GaAs (110) [18]. In addition, the deviation from the reported value may be partially attributed to the simplification of the model in which polarization is approximated to opposite point charges, $\pm q_{\mathrm{dip}}$.

Based on the above analysis in quartz, we estimated the piezoelectric coefficients in soft biological tissues. As seen in Fig. S6, a time delay of $\Delta t \sim 1$ μs is found also in soft biological tissues. Although the mechanical resonance effect is not expected in soft tissues, the acoustically excited area S_{ex} will be larger than the focal spot size due to ultrasound propagation. In this study, we assume that the lateral spread of the focal spot, Δx, is determined by the time constant ($\Delta t \simeq 1.2$ μs) in the detection system (bandwidth of the LCR resonator). Using $S_{\mathrm{ex}} = \pi(\Delta r + \Delta x)^2 = 1.9 \times 10^{-5}$ m^2 and $l = \lambda/2 \sim 0.1$ mm, the piezoelectric coefficient is roughly estimated to be ~ 1 pC/N for Achilles tendon and ~ 2 pC/N for aortic wall.